

PARTICULATE EMISSIONS FROM A HIGHLY BOOSTED GDI ENGINE

F Leach, R Stone

Department of Engineering Science, University of Oxford, UK

D Richardson

Powertrain Research, Jaguar Land Rover, UK

A Lewis, S Akehurst, J Turner

Powertrain & Vehicle Research Centre, University of Bath, UK

S Remmert, S Campbell, R Cracknell

Shell Global Solutions, UK

Abstract

Downsized, highly boosted, GDI engines are becoming the preferred gasoline engine technology to ensure that increasingly stringent fuel economy and emissions legislation are met. The Ultraboost project engine is a 2.0 L in-line 4-cylinder prototype engine, designed to have the same performance as a 5.0 L V8 naturally aspirated engine but with reduced fuel consumption. It is important to examine Particle Number (PN) emissions from such extremely highly boosted engines to ensure that they are capable of meeting current and future emissions legislation. The effect of such high boosting on PN emissions is reported in this paper for a variety of operating points and engine operating parameters.

The effect of engine load, air fuel ratio, fuel injection pressure, fuel injection timing, ignition timing, inlet air temperature, EGR level, and exhaust back pressure have all been investigated. It is shown that PN emissions increase with increases in cooled, external EGR and engine load, and decrease with increases in fuel injection pressure and inlet air temperature. PN emissions are shown to fall with increased exhaust back pressure, a key parameter for highly boosted engines. The effects of these parameters on the particle size distributions from the engine have also been evaluated. Significant changes to the particle size spectrum emitted from the engine are seen depending on the engine operating point. Operating points with a bias towards very small particle sizes were noted.

Introduction

Downsizing engines is one of the key techniques proposed to increase fuel economy and reduce CO₂ emissions from internal combustion engines. Downsizing shifts the speed/load operating point to a more efficient region of the operating map by reducing engine capacity; full load capability is maintained by pressurising the inlet air, generally by turbocharging. Further gains are possible as a result of down-cylindering (leading to friction reductions) and de-throttling at part load. Downsized engines are increasingly available in the market¹, and many further engines are in development^{2,3}.

The engine produced by the Ultraboost project (the UB100)⁴ is designed to be 60 % downsized to achieve a 35 % reduction in fuel consumption and CO₂ emissions. The UB100 engine (an externally boosted version) operates at BMEPs of up to 35 bar, by way of comparison a typical market GDI engine, with a turbocharger and supercharger, today operates at a BMEP of 21.7 bar (VW TSI 1.4), the EB16.4 engine fitted to a Bugatti Veyron (quad-turbocharged) operates at 22.1 bar BMEP⁵, and the Mercedes M133 AMG 2.0 L engine at 28.3 bar BMEP⁶. It is of great importance to confirm that aggressively downsized GDI engines such as UB100 are capable of meeting current and future EU emissions legislation particularly with respect to particle number (PN) limits. The European EU6 emissions legislation is effective currently and mandates a PN limit of 6×10^{11} #/km (with derogation to 6×10^{12} #/km permitted until September 2017)⁷.

Gasoline exhaust aerosols typically show a bilognormal distribution of particulate size with two distinct modes, nucleation and accumulation⁸. Nucleation mode particles are characterised by having a diametric size less than approximately 40 nm, and are roughly spherical. Their formation is thought to occur as the exhaust cools and volatile particles pass from gas phase to a condensed phase in the cool, dilute conditions of engine exhaust. Accumulation mode particles generally lie in the size range 40-200 nm. Their formation is thought to occur when fuel molecules undergo pyrolysis at high temperatures, ultimately producing solid particles with a fractal like shape. Two processes can then cause these particles to grow; firstly gaseous phase species in the exhaust condense and adsorb onto these spherules, causing them to grow; secondly these spherules can agglomerate by colliding and sticking together using a sintering process⁹, which produces particles with a fractal like shape¹⁰. This can clearly be seen in Figure 1, showing a large fractal like shaped accumulation mode particle; of note in this image is that transmission electron microscopy requires a very low pressure, such that it is likely that any volatile species adsorbed onto this particle have evaporated. An example particle size distribution of a gasoline exhaust aerosol from a Naturally Aspirated engine is shown in Figure 2.

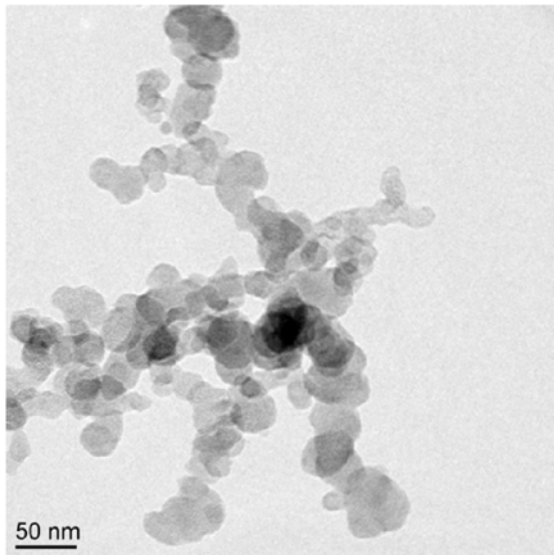


Figure 1: Transmission Electron Microscope image of an accumulation mode particle showing the fractal shape¹¹

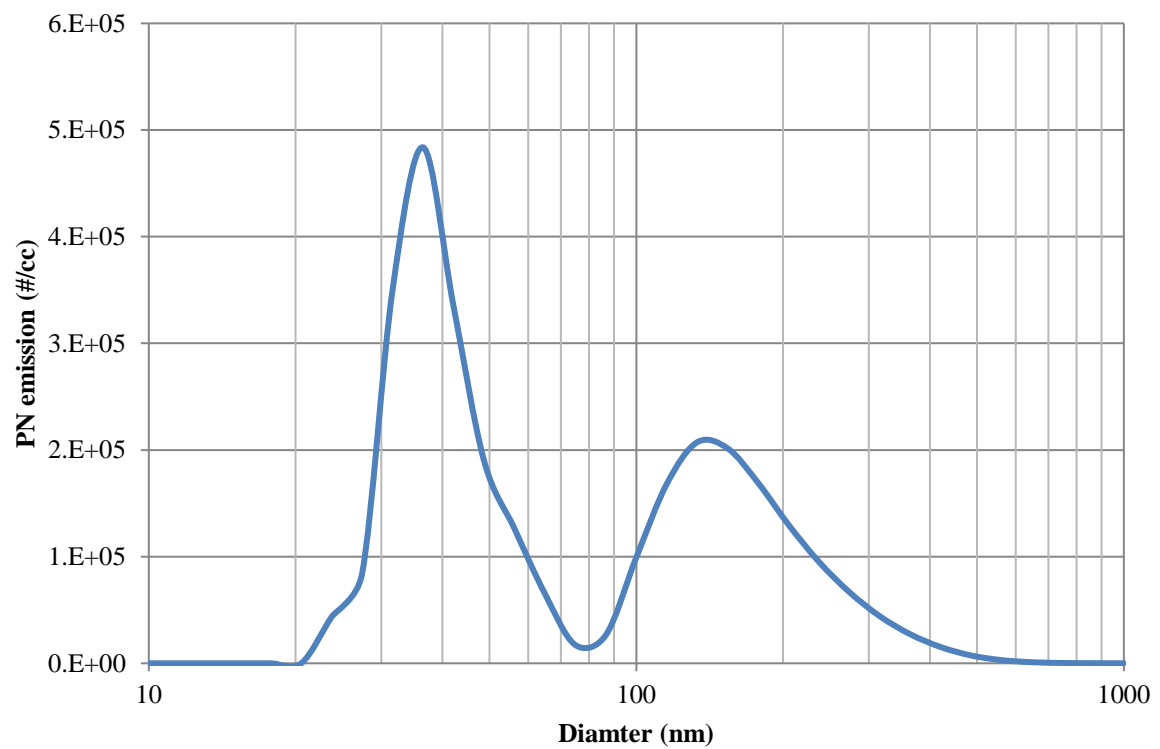


Figure 2: Typical PN size distribution from a naturally aspirated GDI engine showing clear accumulation mode and nucleation mode peaks at c. 35 nm and 120 nm

All of the engine parameters investigated in this work are expected to have an effect on the PN emissions, particulate emissions from an engine this highly boosted have never been reported in the literature, so extrapolation from naturally aspirated and more moderately boosted engines is needed to predict the effect of these parameters. Generally the parameter which is expected to have the largest influence is the air fuel ratio (AFR), where a rich mixture is often observed to give approximately an order of magnitude larger number of particles, compared to the stoichiometric case¹²⁻¹⁵. This is due to a reduction in post-flame soot oxidation.

The effect of increasing the engine load (torque) in GDI engines is generally to increase particulate emissions^{16, 17} because as load increases the amount of fuel present in the cylinder also increases, and with more fuel present, the likelihood of fuel impinging the wall and piston increases, and impinging fuel will burn as a liquid in a pool fire and hence increase the PN emissions. An increase in load will also result in increased in-cylinder pressures during fuel injection on the induction stroke; the increase in cylinder pressure may then result in the fuel penetrating less far into the cylinder before evaporation, resulting in a less homogeneous mixture, and hence higher PN emissions.

The expected effect of spark timing on PN emissions will depend on where the initial ignition timing was. Assuming that the timing is such that the engine is at maximum brake torque (MBT) (the maximum load for a given condition), then deviations from either side of MBT will result in a decrease in particulate emissions, mirroring the effect of engine load on hydrocarbon emissions. Early ignition will lead to there being a longer time for combustion, at lower temperatures and pressures and more time for post flame oxidation, leading to a decrease in PM emissions. Retarding the ignition from MBT increases the exhaust temperature, leading to more post-flame oxidation of particulates, hence a decrease in PM emissions^{14, 17, 18}. For a knock limited operating region (such as would be expected from a highly boosted engine) it can be assumed that the engine will never reach MBT and so it is expected that the effect on PM emissions will be the same as retarding from MBT.

The effect of injection timing on particulate emissions is typically dependent on the engine and load¹⁹⁻²¹, early injection can reduce PN emissions as there is more time for mixture preparation, however too early an injection can result in the fuel impinging on the piston, causing piston wetting and the fuel to burn in a pool fire, resulting in a sharp increase in particulate emissions. It is therefore expected that, depending on the initial timing, load, and engine geometry, an initial fall in PN will be seen, followed by a gentler increase as the injection timing is advanced.

A higher intake air temperature is likely to reduce particulate emissions as there will be better direct injection mixture preparation, as the higher temperatures will promote spray evaporation²². The effect of

increasing EGR levels in GDI engines normally leads to an increase in PN emissions. However, hot EGR can improve mixture preparation, and hence reduce particulate emissions. Therefore the effect of EGR is mixed, and depends on the engine operating point and the levels of EGR^{23, 24}. An increase in exhaust back pressure will increase the residuals present in the cylinder and increase the charge temperature. As was the case for the inlet air temperature, the effect of this is to improve mixture homogeneity. This will lead to a decrease in particulate emissions.

An increase in fuel injection pressure typically promotes better mixture vaporisation and hence reduces particulate emissions, as the higher fuel injection pressures lowers primary droplet sizes in the spray^{15, 21, 25, 26}.

There is no inherent reason why the formulation mechanisms of particulate emissions from a highly boosted engine should be different from their naturally aspirated counterparts. Indeed higher cylinder pressures and temperatures may promote further post-flame oxidation of particulates. However this is not yet demonstrated in the literature. In this work particulate emissions have been sampled from the UB100 Ultraboost 2.0 L i4 engine⁴ using a Cambustion DMS500 in order to evaluate the effect of common engine parameters on PN emissions under extreme boost conditions.

Experimental methodology

The aim of this work was to investigate the effect of key engine operating parameters on PN emissions under highly boosted conditions. The following engine parameters have been chosen for study: load (torque), fuel injection pressure, lambda (λ), inlet air temperature, exhaust gas recirculation (EGR), exhaust back pressure (EBP), fuel injection timing, and ignition timing.

The ‘Ultraboost’ UB100 engine

A comprehensive outline of the UB100 engine concept and design has been given by Turner et al.⁴. The key specifications of the UB100 engine are given in Table 1, and an image of the engine is shown in Figure 3. The aim of the Ultraboost project has been to produce a 2.0 L i4 engine with the same torque curve and power output of the naturally aspirated AJ133 5.0 L V8 engine²⁷. Such aggressive downsizing means that the UB100 operates at a maximum BMEP of 35 bar (AJ133 maximum BMEP is 12.6 bar), and peak cylinder pressures reach 165 bar (AJ133 peak cylinder pressure is 85 bar). Since a robust bottom end was needed, it was expedient to start with the AJ133 V8 engine, and to blank-off and bypass the coolant of one bank of cylinders. The capacity of each cylinder was reduced to 500 cc by fitting a liner, and an entirely new cylinder head was used. The water, oil, and high pressure fuel pumps are all AJ133 production standard components, as are the

main bearings, and fuel injectors (although the maximum fuel injection pressure has been raised slightly from 180 bar to 200 bar).

Table 1: Specifications of the UB100 engine

Type	Inline 4 cylinder
Bore \times Stroke	83 \times 92 mm
Displacement	1991 cm ³
Valves per cylinder	2 intake, 2 exhaust
Compression ratio	9:1
Maximum fuel pressure	200 bar
Peak BMEP	35 bar
Peak cylinder pressure	165 bar

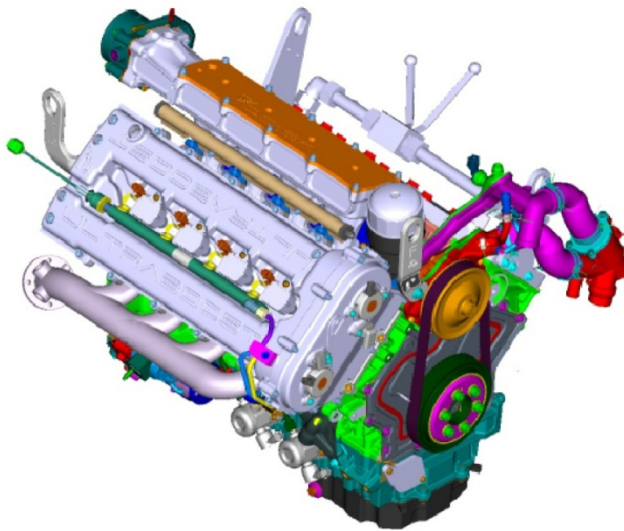


Figure 3: CAD view of the UB100 engine showing AJ133 base engine, new cylinder head, and coolant bypass (adapted from Turner et al.⁴)

The UB100 engine is a ‘proof of concept’ design, and not all of the features of the ultimate engine are included. In particular the turbocharger (which will be a Honeywell GT30) and supercharger (which will be a clutched Eaton R410TVS) are not fitted; rather their functions are provided using an external charging system known as the Combustion Air Handling Unit (CAHU) in conjunction with an Exhaust Back Pressure (EBP) valve.

Instrumentation

The Cambustion DMS500 (DMS) used to measure the particulate emissions from this engine uses electrical mobility measurements of particles to give particle size, number and mass; it is fully described in Reavell *et al.*²⁸. A previous study¹² has shown that using the particle number from the accumulation mode fit (one of the two bilognormal fits that the DMS software outputs automatically) from the DMS500 agrees very well with a Particle Measurement Programme (PMP) legislatively compliant solid particle counting system²⁹ (SPCS) that effectively discounts nucleation mode particles. However, the bilognormal fits need to be used with caution since it is possible for particles that would be considered to be part of the nucleation mode to be assigned to the accumulation mode, and at certain operating conditions this effect was observed in this work. The PMP specifies the use a of a Volatile Particle Remover that eliminates much of the nucleation mode, and regulation compliant particle counters²⁹ are required to have a 50 % count efficiency at $d_p = 23$ nm, and > 90 % count efficiency at $d_p = 41$ nm. This can be modelled using a Wiebe function, with appropriate parameters, as shown in Equation (1), and plotted in Figure 4³⁰.

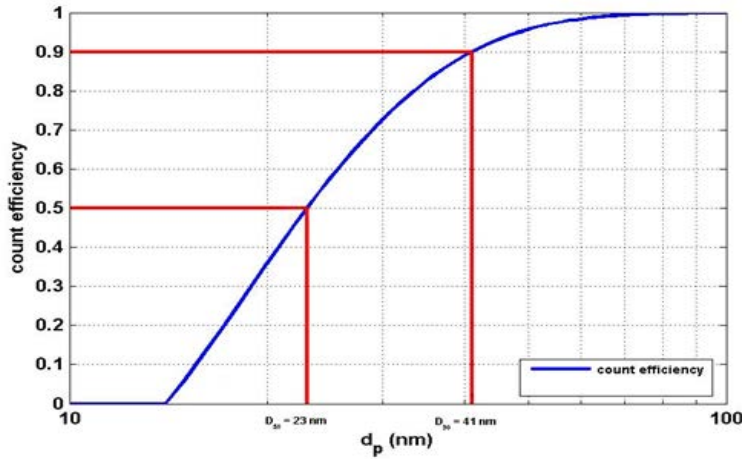


Figure 4: Wiebe function showing a 50 % count efficiency at 23 nm and a 90 % count efficiency at 41 nm (adapted from Leach *et al.*)³⁰

$$f = 1 - \exp \left[-3.54 \left(\frac{d_p - 14}{40} \right)^{1.09} \right], \quad (d_p \geq 14)$$

$$f = 0, \quad (d_p < 14)$$
(1)

This digital filter can be multiplied by the raw particle spectrum which is output from the DMS500. This is an alternative to lognormal fitting, and suppresses the high levels of noise below 23 nm which is

associated with the nucleation mode and are discounted by PMP compliant systems. The results from the DMS have been shown to represent legislatively compliant results closely^{12, 31}. Where particle sizes are presented in this work, they are the mean of the accumulation mode diameter (the DMS measures electrical mobility diameter)²⁸.

For these experiments the sampling location of the DMS500 was approximately 3 m downstream of the exhaust manifold, downstream of the backpressure throttle (used to mimic the effect of a turbocharger) and downstream of one silencer. The first 500 mm of the exhaust manifold is pulse separated and water-cooled (due to the extremely high exhaust temperatures experienced at certain load conditions) and the engine is not fitted with a catalyst. The effect of a catalyst on PN would be to reduce the nucleation mode particles^{18, 32}, which are not being counted here. This water-cooled section is bound to affect the condensation of the volatile particulates, possibly promoting nucleation mode growth; though as already explained, PMP compliant solid particle counting systems do not measure the nucleation mode particles.

Engine test points

The aim was to evaluate the effect of the following engine parameters: load (torque), fuel injection pressure, lambda, inlet air temperature, EGR, EBP, fuel injection timing, and ignition timing. The testing was divided into two phases.

The first phase of testing was to evaluate the effect of engine load and fuel injection pressure on particulate emissions. The engine was run at a fixed speed (2000 rpm) and the load increased from a minimum idling condition, to maximum load at constant speed in nine increments.

The second phase was a large matrix of experiments, shown in Figure 5 and Table 2. At Test Condition 1 (full load, 2000 rpm), a 10 degree spark sweep (from Knock Limited Spark Advance (KLSA), then retarding the spark in increments of 1 degree) was conducted at 0 % and 10 % EGR. At Test Condition 2 (a mapping point used to make predictions of the NEDC performance), an 8 degree spark swing (this Test Condition is not knock limited so KLSA is not applicable), and a 3 point start of injection (SOI) swing was conducted with 20 °C and 40 °C inlet air. At Test Condition 3 (the transition between supercharged and turbocharged operation) a 10 degree spark swing, again from KLSA, was conducted, and the exhaust back pressure was varied to mimic the transition from supercharged operation to turbocharged operation. At Test Condition 4 (full load, 4000 rpm), there was a 3 point spark swing (in this case somewhat retarded from KLSA, and abbreviated to only three points due to engine protection concerns – in particular high exhaust temperature - and lambda was varied from $\lambda = 1.0$ to $\lambda = 0.875$. Test conditions 1,3, and 4 were run by advancing the spark

until either a knock limit was reached (this defined the load for the point marked KLSA on the results graphs) or a cylinder pressure maximum was reached (although the spark advance and load when this point is reached will be different between the parameters varied at each test condition). Test condition 2 was run at fixed load (3.77 bar BMEP).

This test matrix was run in a fixed order: engine stabilisation, 1A, 1B, 2A, 2B, 3A, 3B, 4A, 4B. KLSA was determined by looking at the average knock peak of the four cylinders through a standard AVL algorithm³³. At each test condition the engine was stabilised for 30 s before at least 30 s of DMS data was taken at a sample rate of 10 Hz, downsampled to 1 Hz.

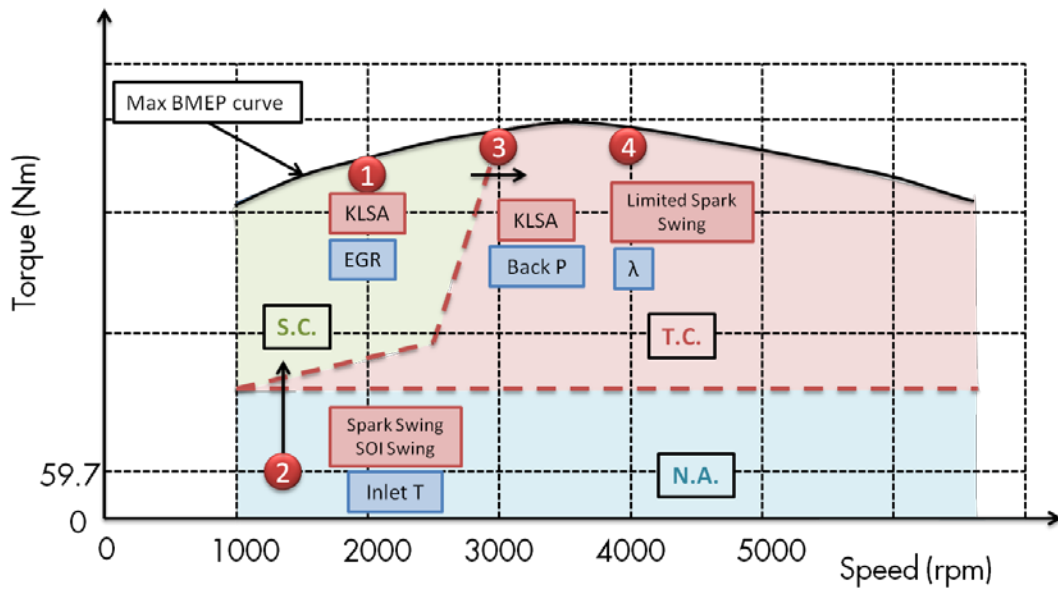


Figure 5: Experimental test conditions run on the UB100 engine

Table 2: Experimental test points for UB100 engine tests

Region	1A	1B	2A	2B	3A	3B	4A	4B
Speed (rpm)	2000		1250		3000		4000	
Initial load	Max BMEP within Knock and P_{max} limits		3.77 bar BMEP (NEDC mini-map point)		Max BMEP within Knock and P_{max} limits		Max BMEP within Knock and P_{max} limits	
Inlet air T (°C)	40		20	40	60		40	
Back P	Low (SC)		Low (NA)		Low (SC)	High (TC)	High (TC)	
EGR (%)	0	10	0		10		10	
λ	1.0		1.0		1.0		1.0	0.875
Fuel injection pressure (bar)	200		60		200		200	
Spark /	KLSA – KLSA-		(1) SOI variation:		KLSA – KLSA-		3 spark points, not as	

injection timing	10 CAD in steps of 1 CAD	± 10 CAD from 330 CAD btdc (2) 8 point spark sweep at 330 CAD btdc SOI	10 CAD in steps of 1 CAD	far as KLSA
	SC – Supercharged	NA – Naturally Aspirated	TC - Turbocharged	

Test fuel

The fuel on which these experiments were conducted was an EN228 compliant gasoline supplied by Shell Global Solutions representative of UK market fuel and as such is an E5 fuel (up to 5 % by volume Ethanol); its specification is shown in Table 3.

Table 3: Ultraboost test fuel specification

RON	MON	RVP (kPa)	FBP (°C)	Ethanol (% v/v)
97	85.3	75.0	188.4	4.91

The results reported here were part of a larger set of experiments testing 14 different fuels, which have been reported elsewhere^{33, 34}. The fuel was tested three times over the course of the experiments. Approximately two experiments were performed per day; and at four instances during the 14 fuel experiments, the engine oil was changed and this was followed by a ‘de-greening’ procedure with four repeats of the complete engine test cycle.

Results and discussion

Effect of engine load on PN emissions

To measure the effect of engine load on PN emissions, the engine was run with a stoichiometric mixture at a fixed speed (2000 rpm), and the load increased in nine increments from ~ 3 to 32 bar BMEP. In order to achieve this load range, the UB100 engine needs to operate in both Naturally Aspirated (NA) and boosted regions of the map, with the turbocharging being mimicked by the CAHU as described above. Given that the UB100 is a prototype engine, it has not been calibrated fully, in particular there is a total change in calibration between the NA and the boosted regions; the result of this is that PN emissions from these two different regions may not be compared directly. In addition to the stepped increase in load, each load point was tested at three injection pressures: 60, 80, and 100 bar in the NA region and 160, 180, and 200 bar in the boosted region. Lower fuel injection pressure reduces the fuel pump work and hence reduces parasitic losses so the influence of fuel injection pressure on PN emissions is of interest.

The results are shown in Figure 6 where it can be seen that the particulate emissions from the UB100 follow the trends seen in other engines¹⁶; that the particulate emissions increase as the load increases. There is over an order of magnitude increase between the lowest and the highest levels of particulates measured. In the boosted region it can be seen that the increase is highly non-linear, with relatively little increase in particulates between 15 & 25 bar BMEP and a step increase between 28 & 32 bar BMEP. The difference that the calibration of the engine makes between the NA and boosted regions can also clearly be seen, with an otherwise unexpected decrease of approximately an order of magnitude in the number of particles counted over the transition (between 10 & 15 bar BMEP). Given that so many engine calibration parameters change (including fuel injection pressure, spark timing, cam lift, cam timing, and injection timing) it is not possible to say which of these has the most effect between the two regions with any certainty.

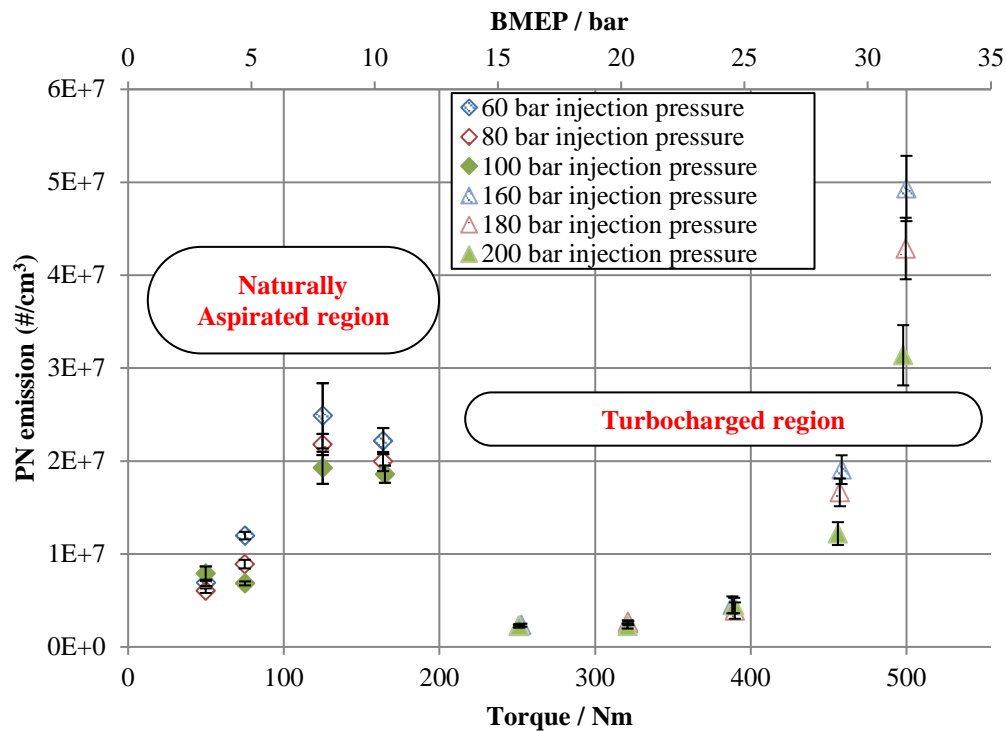


Figure 6: Particulate emissions ($\#/cm^3$) from the UB100 Ultraboost engine as the load is increased from 3 bar BMEP to 32 bar BMEP at a speed of 2000 rpm with a stoichiometric mixture; the error bars correspond to $\pm\sigma$

Figure 7 shows the mean diameter of the accumulation mode particles emitted during the load ramp. In the naturally aspirated region the average diameter of the accumulation mode particles increases with engine load, but is relatively constant with load in the boosted region. By far the biggest influence on particle size comes during the change from naturally aspirated to boosted operation, with the naturally aspirated region

giving smaller particles (as well as fewer particles – see Figure 6). As discussed earlier, so many engine calibration parameters changed that it is impossible to apportion this effect to one parameter in particular. In general terms this can be attributed to there being lower levels of particulates, and therefore fewer primary particles, which can be used as nuclei for accumulation mode particles to agglomerate – leading to a decrease in size.

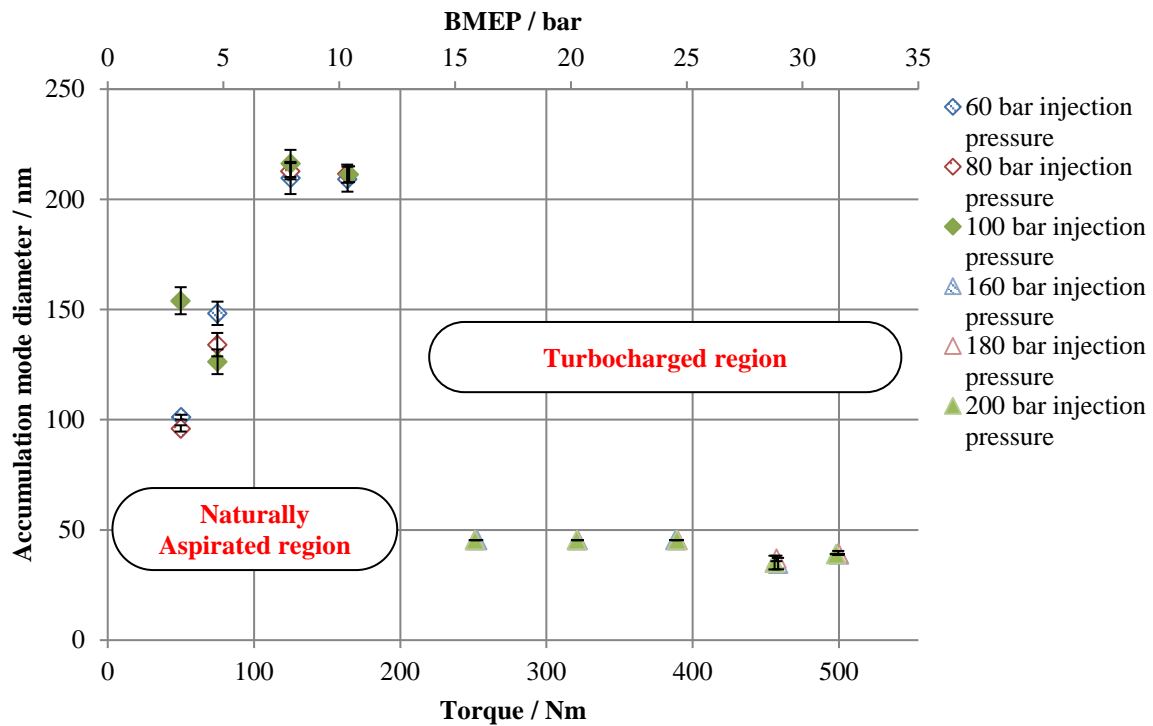


Figure 7: Overall mean accumulation mode particle diameters for the load ramp; it can be seen that in general increasing the fuel pressure decreases the size of the particles emitted; the error bars correspond to $\pm \sigma$

Effect of fuel injection pressure on PN emissions

The effect of fuel pressure on particulate emissions is that the higher the fuel pressure, the lower the particulate emissions; this is a similar result to those reported for NA GDI engines¹⁵. This effect is particularly prominent at higher load conditions for each region, indeed at the maximum load condition increasing the fuel injection pressure from 160 bar to 200 bar reduces the PN emissions by $2 \times 10^7 \text{ \#/cm}^3$, nearly 40%. The effect is also observed at the upper end of the engine's NA region, although a smaller difference in PN emissions than that at full load is observed between injection pressures of 60 & 100 bar. This agrees with the theory that higher fuel pressure results in smaller droplet sizes in the fuel spray, therefore a more homogeneous mixture and hence

lower particulate emissions. Again, fuel injection pressure has a significant impact on particle size with Test Conditions 1, 3, and 4 (Figure 8, Figure 10, and Figure 11), having a fuel injection pressure of 200 bar, and average particle sizes of approximately 40 nm, and Test Condition 2 (Figure 9) having a fuel injection pressure of 60 bar and an average particle size of around 100 nm.

Effect of EGR on PN emissions

Figure 8 shows the PN emissions at Test Condition 1 where the EGR is varied from 0-10 % at 2000 rpm. Here, an increase in EGR leads to a clear increase in PN emissions by up to a factor of two. In these tests the EGR being introduced is cooled low pressure EGR which is externally pumped back into the inlet manifold. As the EGR is both “dry” and “cold”, the heating benefits of high pressure, uncooled EGR are not seen, so any EGR is, in effect, introducing burnt gas, reducing combustion temperatures and hence expansion temperatures leading to less post-flame oxidation and consequently an increase in PN emissions. The effect of EGR independent of exhaust temperature can be examined too in Figure 8. In general adding EGR reduces exhaust temperatures (as expected), however the KLSA point with 0 % EGR and the KLSA – 6° point with 10 % EGR both have exhaust temperatures of 765 °C enabling a direct comparison. This shows a slight decrease in particles at constant exhaust temperature with EGR, which we attribute to the slightly reduced engine load at this condition. Overall, however, the effect of EGR is to increase PN emissions due to reduced exhaust temperature (and hence reduced post-flame oxidation). Increasing EGR from 0-10 % gives an increase in particle diameter of approximately 10 nm – this can be attributed to a general rise in the number of particles as EGR is added, leading to more particles available (due to the decreased exhaust temperature) to agglomerate into larger particles, the size results presented are for the KLSA case.

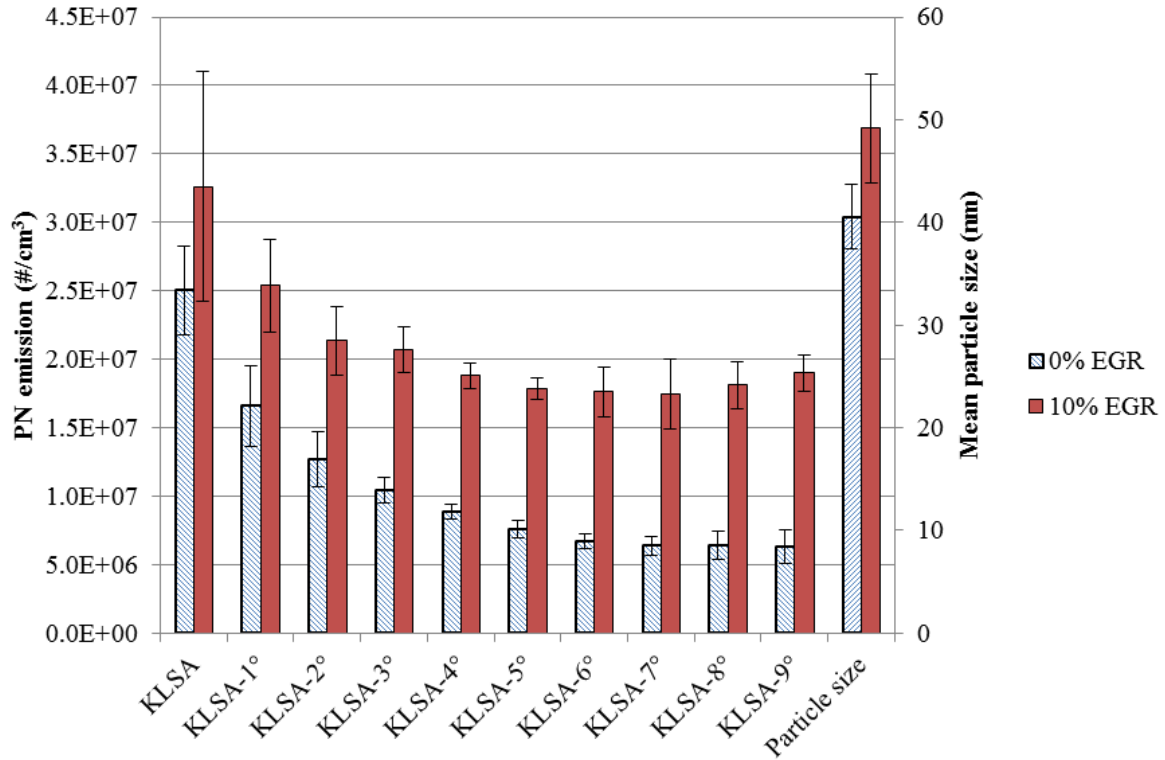


Figure 8: PN emissions at Test Condition 1, a significant increase in PN emissions and mean particle size as the EGR rises from 0-10 % can be seen. The load at KLSA (0% EGR) is 470 Nm; the error bars correspond to $\pm \sigma$

Effect of inlet air temperature on PN emissions

Figure 9 shows the PN emissions at Test Condition 2. As expected, there is a clear trend showing that a higher inlet air temperature leads to a decrease in PN emissions. This is due to a subsequently higher in-cylinder temperature at the point of fuel injection, promoting spray evaporation, leading to a better prepared (more homogeneous) fuel-air mixture and hence lower PN emissions. In addition the overall particulate levels are high (the highest of all the test conditions except the rich condition) despite the low engine load, this is due to the low fuel injection pressure of 60 bar, whereas a fuel injection pressure 200 bar is used for all other test conditions in phase 2. A decrease in mean size of particles is seen as the inlet air temperature is increased again likely due to an overall fall in particle levels resulting in fewer primary particles available to agglomerate into larger particles, the size results presented are for the nominal spark timing case.

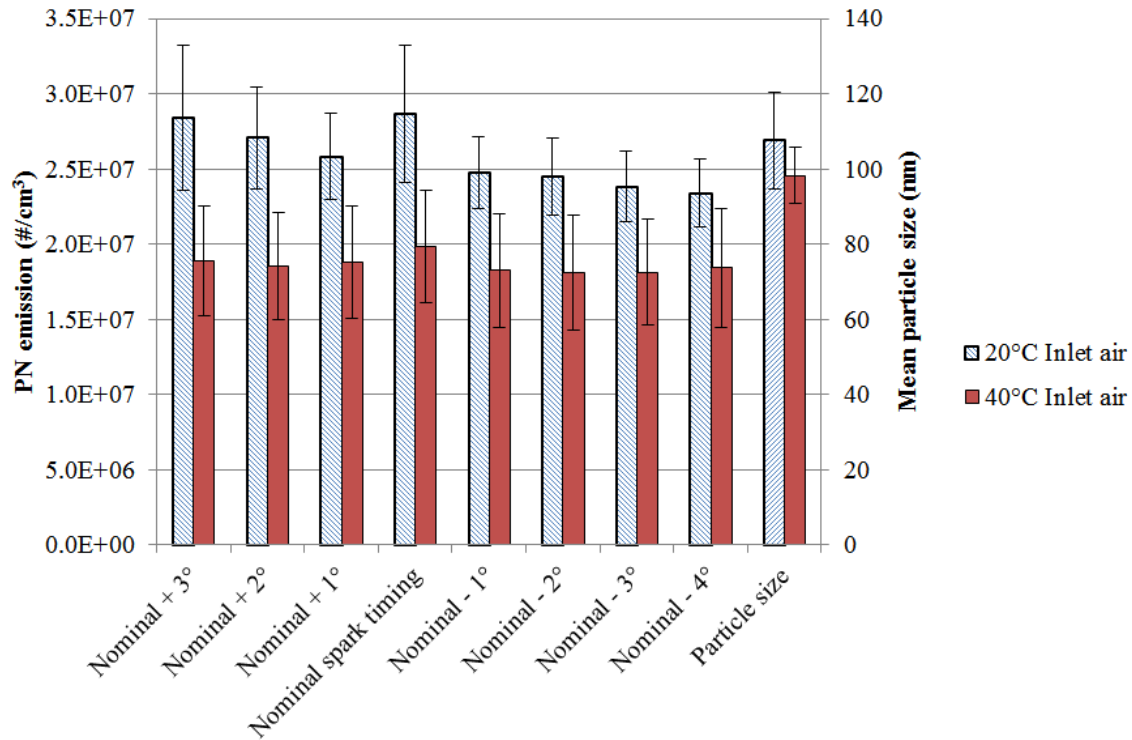


Figure 9: PN emissions at Test Condition 2, a clear decrease in PN emissions and mean particle size as the inlet air temperature is increased can be seen; the error bars correspond to $\pm \sigma$

Effect of exhaust back pressure on PN emissions

Figure 10 shows the PN emissions at Test Condition 3. At and close to KLSA, the effect is significant, with an increase in Exhaust Back Pressure (EBP) leading to a decrease in PN emissions. This shows that an increase in EBP which leads to an increase in in-cylinder residuals, and hence a higher charge temperature, gives improved mixture preparation and therefore lowers PN emissions (this is the same effect as increasing the inlet air temperature). An increase in EBP on this engine also leads to a slight increase in the exhaust temperature (from 788 °C to 802 °C at KLSA), also suggesting greater post-flame oxidation and a reduction in particulates. However, as the spark is retarded from KLSA, the increase in EBP (which is mimicking the transition from supercharged to turbocharged operation) has much less of an effect on PN emissions. This increase in EBP is due to the pressure drop that occurs across a turbocharger (driven by engine exhaust gas) compared to none across a supercharger (driven directly from the engine, and therefore with no direct impact on exhaust pressure)³⁵. This suggests that the increase in exhaust temperature (a much greater increase than with change of EBP only) seen with retarding from KLSA is a more dominant effect than EBP itself once sufficiently

retarded from KLSA. In addition, no significant change in particle size is observed with EBP (the size results presented are for the KLSA case).

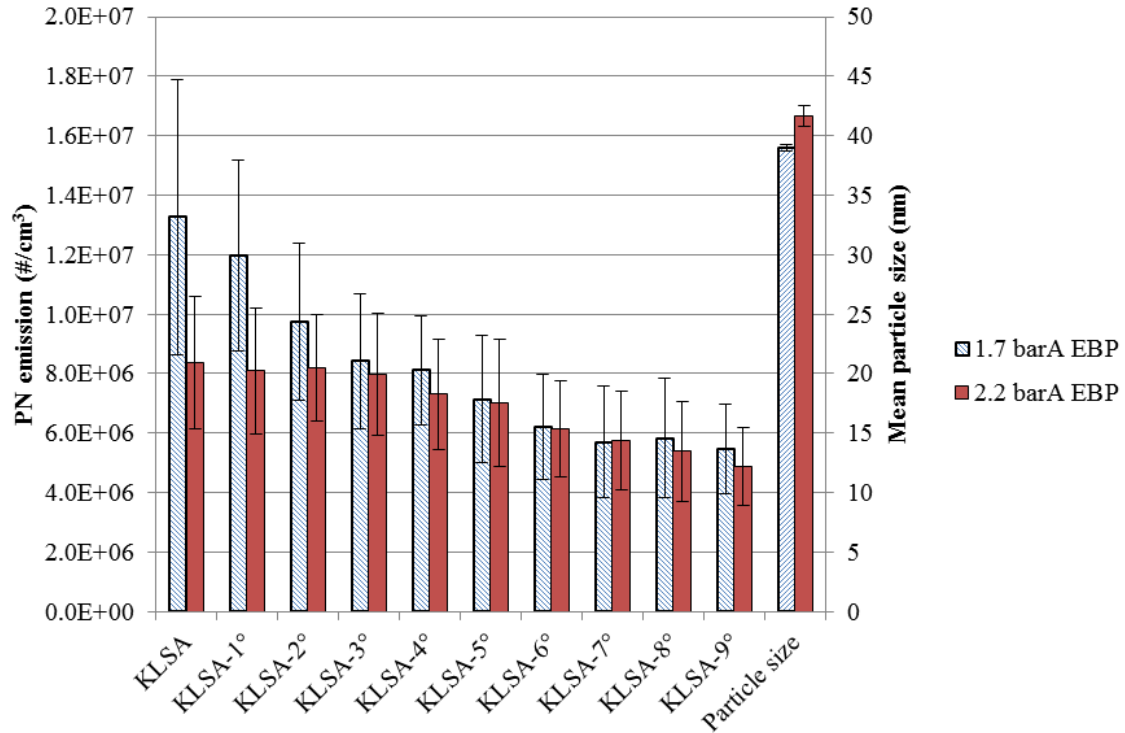


Figure 10: PN emissions at Test Condition 3, showing that close to KLSA there is a significant decrease in PN with increased Exhaust Back Pressure (EBP) but as the ignition timing retards from KLSA the effect is reduced, a small increase in particle size is also observed; the error bars correspond to $\pm \sigma$

Effect of lambda on PN emissions

Figure 11 shows the PN emissions at Test Condition 4. Figure 11 shows clearly what is well known in the literature that as lambda changes from stoichiometric to rich ($\lambda = 1.0$ to $\lambda = 0.875$) the particulate emissions increase drastically. It can also be seen that the repeats give very similar PN levels, again giving confidence about the repeatability of the results. There is no significant change in mean particle size observed with varying λ , increasing lambda increases overall PN emissions significantly, but has no effect on the particle size distribution (the size results presented are for the spark timing 1 case).

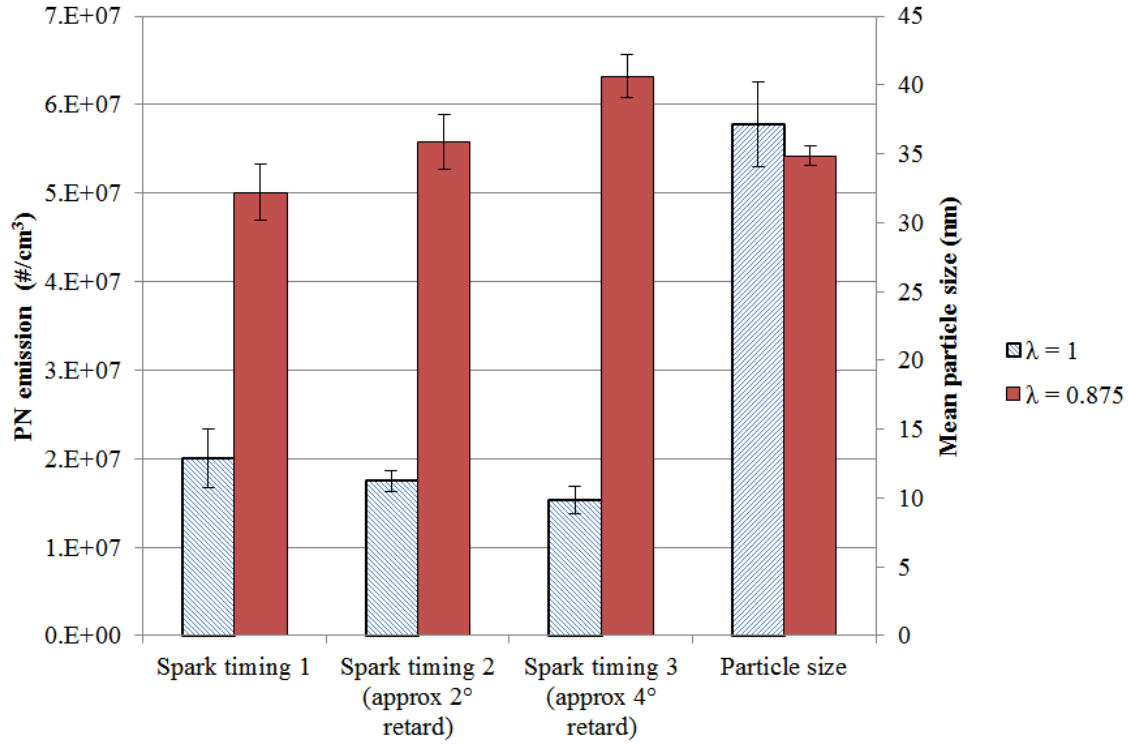


Figure 11: PN emissions at Test Condition 4, strong agreement with the hypothesis that PN should increase as the mixture becomes rich can be seen, no significant change in mean particle size is observed; the error bars correspond to $\pm \sigma$

Effect of ignition timing on PN emissions

Retarding the spark (ignition) timing from MBT or KLSA should decrease particulate emissions because retarding the ignition timing will increase the exhaust temperature, which will promote post flame oxidation of particulates.

Figure 8, Figure 9, Figure 10, and Figure 11 all show PN emissions from spark swings. In general these figures show that the PN emissions decrease as the spark timing is retarded, as expected. At Test Condition 2, (Figure 9) there is almost no difference in PN with spark timing; this is because the engine is operating at such light load, that the effects of a spark swing on PN are negligible. At Test Condition 4 (Figure 11) when the mixture is rich, retarding the spark led to an increase in PN emissions; this can be explained as there is so much fuel present, that there is simply not enough air present to burn all of the fuel and a reduction in the time available for combustion (by retarding the spark) leads to the increase in PN emissions as there is no post-flame oxidation. Ignition timing was observed to have little effect on the mean particle size so for clarity, these results are omitted from the figures. It is also of note that comparing Figure 6 and Figure 8, taken at the

same engine speed and broadly the same load (470 Nm at KLSA in Figure 8 and up to 500 Nm in Figure 6), that a larger decrease in PN can be obtained by retarding ignition by say two degrees compared with reducing fuel injection pressure. This suggests that all other things being equal, retarding ignition would be a more effective PN reduction strategy (although this would incur a load penalty). More experiments would need to be conducted to prove this effect however.

Effect of fuel injection timing on PN emissions

Considering the impact of fuel injection timing on particulate emissions, there is a balance between a retarded injection reducing the time for fuel preparation, and hence increasing PN emissions, and a retarded injection reducing fuel impingement on the piston, which will act to decrease PN emissions. Given the step change in emissions that arises from piston wetting compared with the less dramatic (but more continuous) change from decreased mixture preparation time, and considering the very early injection timing (see the following paragraph) it would be expected that the PN emissions would initially decrease as the injection timing was retarded as with this early injection timing, fuel impingement is likely. As the injection timing is further retarded a rise in PN emissions would be expected as there is less time available for fuel evaporation.

Three test points tested the fuel injection timing, and the injection timing at these points was 340, 330, and 320° btdc. Fuel injection timings were kept constant for all of the fuels tested (although these other fuels are not reported here). These timings are very early injection timing for a GDI engine (280° btdc might be expected), even for homogeneous operation, but this was chosen to ensure that enough fuel for stoichiometric operation could be injected at high engine speed, particularly with high oxygenate content blends (although these fuels are not reported in this work).

Figure 12 shows that at injection timings of 340 and 330° btdc the PN emissions are very similar (for a given inlet air temperature, discussed elsewhere in this paper), but at an injection timing of 320° btdc there is a clear reduction in PN emissions (by over a factor of two). This suggests significant fuel impingement (the fuel injection is happening when the piston is very close to tdc), and that at 320° btdc (once the piston has moved away from tdc) this is no longer happening, leading to this significant reduction in PN emissions.

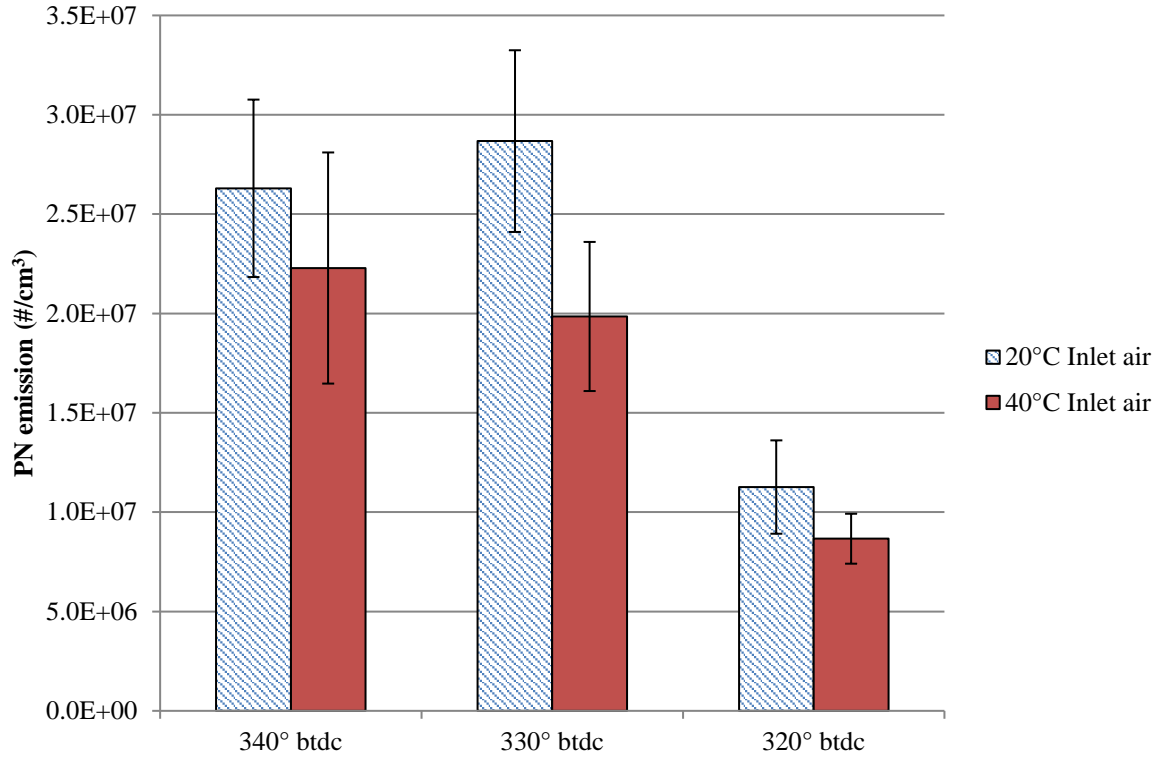


Figure 12: PN emissions at Test Condition 2 varying fuel injection timing. It can clearly be seen that increasing the inlet air temperature reduces PN due to better mixture preparation, and that later injection reduces PN – due to a reduction in fuel impingement; the error bars correspond to $\pm \sigma$

Conclusions

An extensive test matrix of 96 test points has been undertaken on an extremely highly boosted engine, across the engine map at operating points of up to 32 bar BMEP. The particulate emissions have been measured from this engine for the first time, using a DMS500.

The effect of engine load on PN emissions in both the naturally aspirated and boosted regions has been measured and the results show that the PN emissions increase with load, and decrease with increased fuel pressure. Increasing fuel injection pressure is an effective strategy for reducing particulate emissions from highly boosted gasoline engines, however higher fuel pressures require more power to be delivered to the fuel pump(s), which increases specific fuel consumption and CO₂ emissions so a compromise between these two demands is needed.

The effects of spark timing, fuel injection timing, inlet air temperature, exhaust back pressure, EGR, and lambda on PN emissions have also been measured. These results are presented in summary form in Table 4.

The most significant effects have been seen with varying Lambda (a well-established result for GDI engines at lower boost levels) and EGR (here cooled, low pressure, dry EGR).

Table 4: Summary results for the engine parameters tested in this work

Variable	Hypothesis	Comment
Engine load	Load \uparrow Particulates \uparrow	As load increases the amount of fuel present in the cylinder also increases leading to an increase in PN emissions
Fuel injection pressure	P \uparrow Particulates \downarrow	An increase in fuel injection pressure will result in lower droplet size and hence improved mixture preparation and so decrease PN emissions as well as particle size
EGR	EGR \uparrow Particulates \uparrow	An increase in cooled/external EGR will increase PN emissions
Inlet air temperature	T \uparrow Particulates \downarrow	An increase in inlet air temperature will result in improved mixture preparation and so decrease PN emissions
Exhaust back pressure	Back pressure \uparrow Particulates \downarrow	An increase in exhaust back pressure increases the (hot) residuals, which increases the mixture temperature, this improves mixture homogeneity and leads to a decrease in PN emissions
λ (AFR)	λ \downarrow Particulates \uparrow	A decrease in λ leads to an increase in PN emissions ($\lambda = 1.0 - \lambda = 0.875$), this is a well-documented effect ¹²
Spark timing	Ignition \leftarrow Particulates \downarrow	Retarding the spark from MBT increases post-flame oxidation and reduce PN emissions
Fuel injection timing	Injection \rightarrow Particulates \downarrow	Moving the fuel injection away from tdc reduces spray impingement and hence reduces PN emissions (this effect holds until reduced mixture preparation time results in poorly prepared mixtures leading to higher PN)

The effect of those parameters on PN size distributions has also been measured. On the whole the effect of these parameters on PN size distributions is lower than on the overall PN emission levels, but there are clear trends observed for inlet air temperature and EGR in line with the theory. Lambda and EBP have little effect on engine size distributions.

PN emissions are a legislated parameter in Europe, and knowledge of their formation under highly boosted conditions is particularly important given the increasing deployment of downsized (and hence highly boosted) GDI engines in the market. This study confirms that PN emission trends from highly boosted GDI engines follow that of their moderately boosted and naturally aspirated counterparts. Parameters of particular

importance for highly boosted engines (such as Exhaust Back Pressure) have been shown to decrease PN emissions which reduces as ignition timing is retarded from KLSA, these effects will need to be carefully monitored by engine calibrators as highly boosted engines gain further market share.

Acknowledgments

The authors acknowledge the Technology Strategy Board (now Innovate UK), the UK's innovation agency, for the partial funding of this work. Consortium members GE Precision Engineering, Lotus Engineering, CD Adapco, Imperial College London, and the University of Leeds have all made various portions of this work possible.

Funding

This work was funded by Jaguar Land Rover, Shell, the Technology Strategy Board, and all of the project partners listed above made contributions. Felix Leach acknowledges the support of an EPSRC studentship.

References

1. Friedfeldt R, Zenner T, Ernst R and Fraser A. Three-Cylinder Gasoline Engine with Direct Injection. *Auto Tech Review*. 2013; 2: 32-7.
2. Martin, S., Beidl, C., and Mueller, R. Responsiveness of a 30 Bar BMEP 3-Cylinder Engine: Opportunities and Limits of Turbocharged Downsizing. SAE Technical Paper 2014-01-1646, 2014, doi:10.4271/2014-01-1646.
3. Hancock, D., Fraser, N., Jeremy, M., Sykes, R. et al. A New 3 Cylinder 1.2l Advanced Downsizing Technology Demonstrator Engine. SAE Technical Paper 2008-01-0611, 2008, doi:10.4271/2008-01-0611.
4. Turner, J., Popplewell, A., Patel, R., Johnson, T. et al. Ultra Boost for Economy: Extending the Limits of Extreme Engine Downsizing. *SAE Int. J. Engines* 7(1):387-417, 2014, doi:10.4271/2014-01-1185.
5. Herdin G. The Engine World and their "Reccords" [sic]. *HTL Vortragsreihe "neue Technologien und Innovationen"*. Steyr 2012.
6. Webpage AMG 2.0-LITER INLINE 4 TURBO ENGINE, <http://www.mercedes-amg.com/> (2016, accessed 17 March 2017).
7. Commission Regulation 692/2008, OJ L 199 of 18.7.2008.
8. Eastwood P. *Particulate Emissions from Vehicles*. SAE International and John Wiley & Sons, Ltd., 2008.
9. Eggersdorfer ML and Pratsinis SE. The Structure of Agglomerates Consisting of Polydisperse Particles. *Aerosol Science and Technology*. 2011; 46: 347-53.
10. Eggersdorfer ML, Kadau D, Herrmann HJ and Pratsinis SE. Multiparticle Sintering Dynamics: From Fractal-Like Aggregates to Compact Structures. *Langmuir*. 2011; 27: 6358-67.
11. Price P. Direct injection gasoline engine particulate emissions. *DPhil Thesis, Engineering Science*. Oxford, 2009.
12. Braisher, M., Stone, R., and Price, P. Particle Number Emissions from a Range of European Vehicles. SAE Technical Paper 2010-01-0786, 2010, doi:10.4271/2010-01-0786.
13. Leach, F., Stone, R., and Richardson, D. The Influence of Fuel Properties on Particulate Number Emissions from a Direct Injection Spark Ignition Engine. SAE Technical Paper 2013-01-1558, 2013, doi:10.4271/2013-01-1558.

14. Price, P., Twiney, B., Stone, R., Kar, K. et al. Particulate and Hydrocarbon Emissions from a Spray Guided Direct Injection Spark Ignition Engine with Oxygenate Fuel Blends. SAE Technical Paper 2007-01-0472, 2007, doi:10.4271/2007-01-0472.
15. He X, Ratcliff MA and Zigler BT. Effects of gasoline direct injection engine operating parameters on particle number emissions. *Energy & Fuels*. 2012; 26: 2014-27.
16. Kittelson DB. Engines and nanoparticles: a review. *Journal of Aerosol Science*. 1998; 29: 575-88.
17. Farron, C., Matthias, N., Foster, D., Andrie, M. et al. Particulate Characteristics for Varying Engine Operation in a Gasoline Spark Ignited, Direct Injection Engine. SAE Technical Paper 2011-01-1220, 2011, doi:10.4271/2011-01-1220.
18. Chen, L., Braisher, M., Crossley, A., Stone, R. et al. The Influence of Ethanol Blends on Particulate Matter Emissions from Gasoline Direct Injection Engines. SAE Technical Paper 2010-01-0793, 2010, doi:10.4271/2010-01-0793.
19. Pei Y-Q, Qin J and Pan S-Z. Experimental study on the particulate matter emission characteristics for a direct-injection gasoline engine. *Proceedings of the Institution of Mechanical Engineers, Part D: Journal of Automobile Engineering*. 2014; 228: 604-16.
20. Qin, J., Li, X., and Pei, Y. Effects of Combustion Parameters and Lubricating Oil on Particulate Matter Emissions from a Turbo-Charged GDI Engine Fueled with Methanol/Gasoline Blends. SAE Technical Paper 2014-01-2841, 2014, doi:10.4271/2014-01-2841.
21. Cho J, Si W, Jang W, Jin D, Myung C-L and Park S. Impact of intermediate ethanol blends on particulate matter emission from a spark ignition direct injection (SIDI) engine. *Applied Energy*. 2015; 160: 592-602.
22. Maurya RK, Agarwal AK. Effect of intake air temperature and air-fuel ratio on particulates in gasoline and n-butanol fueled homogeneous charge compression ignition engine. *International Journal of Engine Research*. 2014 Oct;15(7):789-804.
23. Ladommatos N, Abdelhalim S and Zhao H. The effects of exhaust gas recirculation on diesel combustion and emissions. *International Journal of Engine Research*. 2000; 1: 107-26.
24. Hedge, M., Weber, P., Gingrich, J., Alger, T. et al. Effect of EGR on Particle Emissions from a GDI Engine. *SAE Int. J. Engines* 4(1):650-666, 2011, doi:10.4271/2011-01-0636.
25. Hoffmann, G., Befrui, B., Berndorfer, A., Piock, W. et al. Fuel System Pressure Increase for Enhanced Performance of GDI Multi-Hole Injection Systems. *SAE Int. J. Engines* 7(1):519-527, 2014, doi:10.4271/2014-01-1209.
26. Elkotb MM. Fuel atomization for spray modelling. *Progress in Energy and Combustion Science*. 1982; 8: 61-91.
27. Sandford, M., Page, G., and Crawford, P. The All New AJV8. SAE Technical Paper 2009-01-1060, 2009, doi:10.4271/2009-01-1060.
28. Reavell, K., Hands, T., and Collings, N. A Fast Response Particulate Spectrometer for Combustion Aerosols. SAE Technical Paper 2002-01-2714, 2002, doi:10.4271/2002-01-2714.
29. Andersson J, Giechaskiel B, Muñoz-Bueno R, Sandbach E and Dilara P. Particle Measurement Programme (PMP) Light-duty Inter-laboratory Correlation Exercise (ILCE_LD) Final Report. European Commission Joint Research Centre Institute for Environment and Sustainability, 2007.
30. Leach F. Particulate Emissions from Gasoline Direct Injection engines. *DPhil Thesis, Engineering Science*. University of Oxford, 2014.
31. Leach F, Stone R, Fennell D, Hayden D, Richardson D and Wicks N. Predicting the particulate matter emissions from spray-guided gasoline direct-injection spark ignition engines. *Proceedings of the Institution of Mechanical Engineers, Part D: Journal of Automobile Engineering*. First published date: September-30-2016, doi:10.1177/0954407016657453.
32. Peckham, M., Finch, A., Campbell, B., Price, P. et al. Study of Particle Number Emissions from a Turbocharged Gasoline Direct Injection (GDI) Engine Including Data from a Fast-Response Particle Size Spectrometer SAE Technical Paper 2011-01-1224, 2011, doi:10.4271/2011-01-1224.
33. Remmert, S., Campbell, S., Cracknell, R., Schuetze, A. et al. Octane Appetite: The Relevance of a Lower Limit to the MON Specification in a Downsized, Highly Boosted DISI Engine. *SAE Int. J. Fuels Lubr*. 7(3):743-755, 2014, doi:10.4271/2014-01-2718.
34. Remmert, S., Cracknell, R., Head, R., Schuetze, A. et al. Octane Response in a Downsized, Highly Boosted Direct Injection Spark Ignition Engine. *SAE Int. J. Fuels Lubr*. 7(1):131-143, 2014, doi:10.4271/2014-01-1397.
35. Stone CR. *Introduction to Internal Combustion Engines*. 4th ed. Palgrave Macmillan, 2012.